Ray-Tracing Analysis of the Near and Far Fields of Focusing Geodesic Lens Antennas

Germán León*, Omar Orgeira†, Nelson J. G. Fonseca‡, Oscar Quevedo-Teruel§
*Dept. of Electrical Engineering, Universidad de Oviedo, Gijón, Spain, gleon@uniovi.es
†Universidad de Oviedo, Gijón, Spain, omarorgeira@gmail.com
‡Antenna and Sub-Millimetre Waves Section, European Space Agency, Noordwijk, The Netherlands, nelson.fonseca@esa.int
§Divison of Electromagnetic Engineering, KTH Royal Institute of Technology, Stockholm, Sweden, oscarqt@kth.se

***Abstract*—Geodesic lenses are a class of rotational-symmetric lenses that recently regained interest for the design of multiple beam antennas. Key features of these lenses include mechanical simplicity, wide scanning range and high efficiency. In this paper, a hybrid model to analyze focusing geodesic lens antennas is described. The method combines a ray tracing analysis and a point source array model. This model allows to calculate the near and far fields of a geodesic lens antenna in few seconds. Some results of a lens antenna in the Ka-band are compared with full-wave simulations, validating the model despite small differences in the main beam. This paper also discusses the ability of geodesic lenses to focus the energy in the near field which could be of interest for some applications.**

***Index Terms*—Lens antennas, geodesic lenses, parallel plate waveguide, ray-tracing, near and far fields analysis, multiple beam antennas.**

I. Introduction

Next generation communication satellites [1] and future 5G mobile networks [2], [3] require higher data rates and low cost antenna systems. Multiple beam antennas based on lenses can fulfill these requirements at mm-wave frequencies while covering a wide field of view [4]. These antennas may generate multiple simultaneous beams from a same aperture, subdividing the service area and enabling spectrum re-use in non-adjacent cells.

For some applications, a planar (e.g. azimuthal) beam scanning is sufficient. Rotman lens antennas [5] manufactured in printed technology are reported in the literature for such applications with a scan angle of about $\pm 30°$ [6], [7]. Although attractive for their low cost, these solutions suffer from high losses due to the use of dielectric materials inside the lens. Fully-metallic parallel plate waveguide (PPW) technology is preferred at mm-wave frequencies. In [8], [9], the authors present a ray-tracing analysis of a continuous PPW beam-former based on the propagation inside a transversal cavity operating as a continuous delay lens. This solution is attractive for its mechanical simplicity. However, its scanning range remains in the order of $\pm 30°$. Rotman lenses may be modified to extend their scanning range to about $\pm 50°$ [10]. Beyond that, only Luneburg lenses [11] provide suitable scanning properties thanks to their inherent rotational symmetry. Various designs of Luneburg lens antennas were recently investigated [12]-[15]. These antennas demonstrate good scanning properties up to $\pm 60°$. The designs in [12]-[14] rely on sub-wavelength elements (e.g. holes or pins) to emulate the behavior of the reference Luneburg lens, resulting in mechanical complexity and higher manufacturing cost. The design reported in [15] is a lot simpler but it uses the dispersive behavior of the TE mode in a PPW cavity. Hence, its operation is inherently limited in bandwidth. In this context, geodesic lenses, and in particular, the Rinehart-Luneburg lens [16], [17], are attractive solutions since they combine both mechanical simplicity and true-time-delay operation. Recent works have investigated the possibility to fold or modulate the profile of geodesic lenses to reduce their height [18]-[20]. To further investigate these solutions, there is an interest in developing efficient analysis tools enabling a quick assessment of the focusing properties of geodesic lenses.

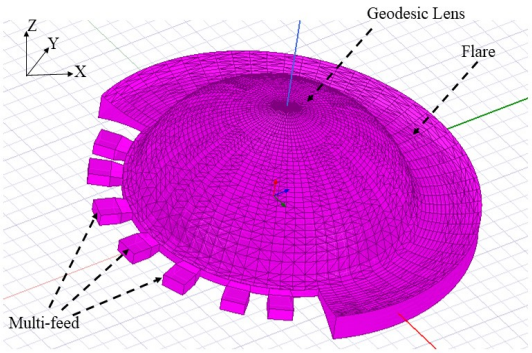

Fig. 1. 3D view of a focusing geodesic lens antenna.

In this contribution, a hybrid model to analyze geodesic lenses is described. The model uses a ray-tracing method to evaluate the path of the rays inside the lens. The radiation patterns in the far field (FF) and near field (NF) of the lens are studied using a point source array approximation. In particular, geodesic lenses with NF focusing properties are investigated. The model provides more incite in the focusing properties of such lenses.

II. Focusing Geodesic Lens Design

In Fig. 1, a 3D view of a focusing geodesic lens antenna is presented. A TEM wave, generated by a waveguide feed, travels through a curved PPW cavity. The lens antenna opens smoothly to the open space through a flare on the opposite side of the feeds. The geodesic lens presents a rotational symmetry around the Z-axis, providing the desired stability of focusing properties across a wide angular range, only limited by the implementation of the feeds. This structure can be modeled (Fig. 2) as a point source at the position, $P_1(\rho_1 = 1, \theta_1 = -\pi)$, from where several rays emerge, travel on a geodesic surface and focus at the point $P_2(\rho_2, \theta_2 = 0)$, where ρ is the radial coordinate normalized to the lens radius (R_{lens}) and θ the angular position with reference to the X-axis in the XOZ plane.

The optimal contour of a geodesic lens can be calculated using the function $s(\rho)$ [21], the length of surface measured along the meridian from the axis Z to a given point:

$$s(\rho) = A(\rho)\rho + B\arcsin(\rho) + C(\rho) \tag{1}$$

where

$$A(\rho) = 1 - \frac{1}{\pi}\arcsin\sqrt{\frac{1-\rho^2}{\rho_2^2-\rho^2}} \tag{2}$$

$$B = \frac{1}{\pi}\arcsin\frac{1}{\rho_2}. \tag{3}$$

$$C(\rho) = -\frac{\rho_2}{\pi}\arcsin\sqrt{\rho\frac{\rho_2^2-1}{\rho_2^2-\rho^2}}. \tag{4}$$

This equation ensures that all rays emerging from P_1 arrive at P_2 traveling the same distance, thus adding up in phase. The value of P_2 varies from $r_2 = 1$ (Maxwell fish eye lens) to $r_2 = \infty$ (Rinehart-Luneburg lens). Some examples are plotted in Fig. 3.

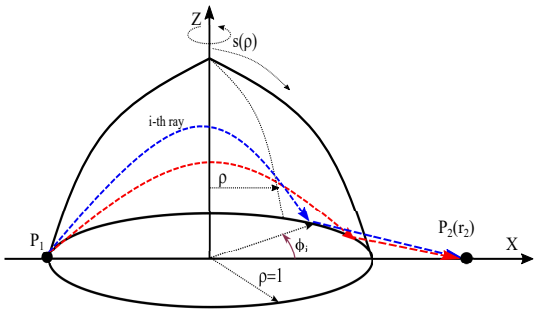

Fig. 2. Schematic representation of ray tracing in a geodesic lens.

III. Point Source Circular Array Model

A ray tracing tool has been developed, following the equations described in [21], to calculate the total length travel by the ray (σ_i) and the angle of arrival at the end of the lens (ϕ_i). Each ray arrives at that point forming an angle θ_i with the X-axis. The lens aperture can be modeled as a point source array, where each source radiates proportional to $cos^p(\theta - \theta_i)$.

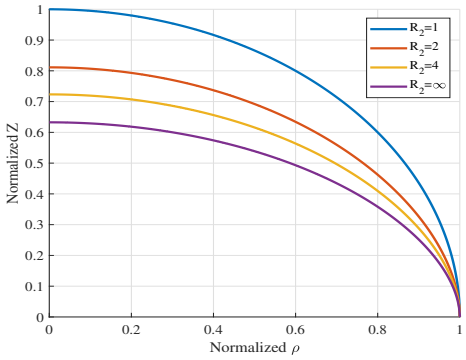

Fig. 3. Different lens profiles as a function of the radial position of the image focusing point.

The electric field created by the lens antenna in the point $(\bar{x}, \bar{y})$, normalized to the wavelength, can be calculated as the sum of the contributions of all the point sources.

$$E_z(\bar{x}, \bar{y}, \bar{z} = 0) \propto \sum_{i=1}^{n} \cos^q(\alpha_0^i) \cdot exp(-j2\pi\sigma_i) \cdot exp(-j2\pi R) \cdot \cos^p(\theta - \theta_i)/R_i \tag{5}$$

where

$$R_i = \sqrt{(\bar{x} - R_{lens}\cos\phi_i)^2 + (\bar{y} - R_{lens}\sin\phi_i)^2}). \tag{6}$$

The source in P_1 is modeled as a $cos^q(\alpha_0^i)$ feed, with α_0^i the angle between the emerging ray and the meridian of the lens. This simplified model provides an efficient analysis tool and better insight on the operation of a geodesic lens. The model requires only a few seconds to provide the radiation pattern of the antenna in a laptop.

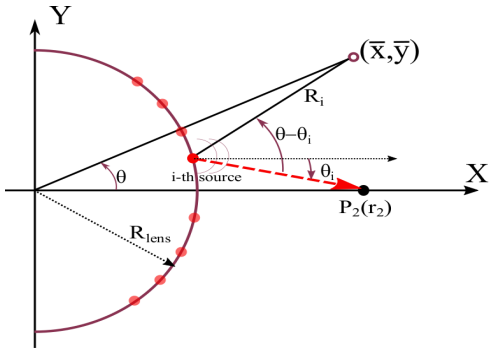

Fig. 4. Schematic representation of the point source circular array model.

IV. Validation of the Hybrid Model

A. Pattern Analysis

A specific geodesic lens antenna is defined with the purpose of comparing the results from the hybrid model described above and a commercial full-wave tool [23]. The geodesic lens has a radius of $R_{lens} = 4\lambda$ and the working frequency is 30 GHz. The focusing point is $r_2 = 4 \cdot R_{lens} = 160$ mm.

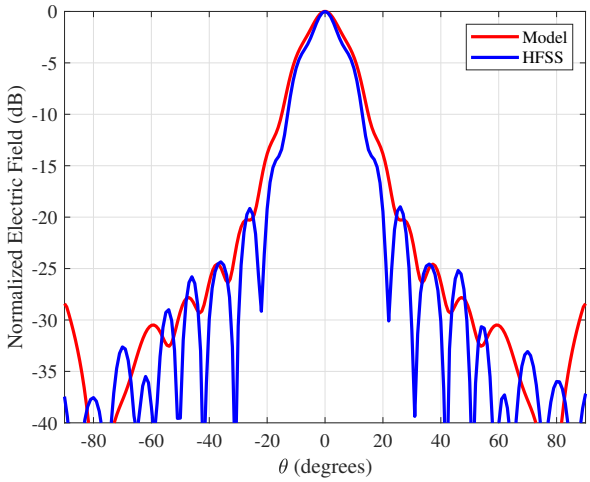

Fig. 5. Far field radiation pattern of a geodesic lens antenna $R_{lens} = 4 \cdot \lambda$ and $r_2 = 4 \cdot R_{lens}$.

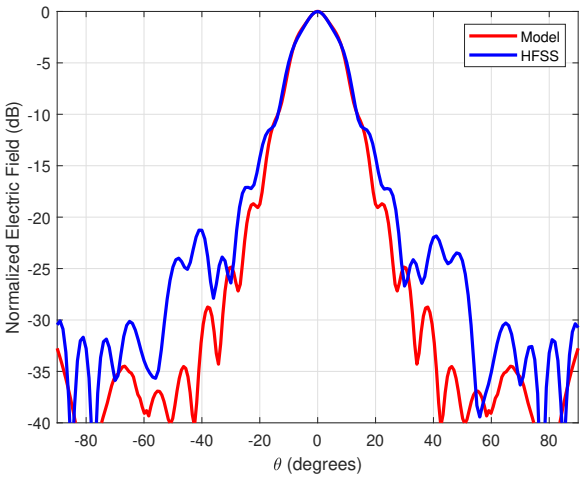

Fig. 7. Normalized NF pattern at $R = 2 \cdot R_{lens}$ of a geodesic lens antenna with $R_{lens} = 4 \cdot \lambda$ and $r_2 = 4 \cdot R_{lens}$.

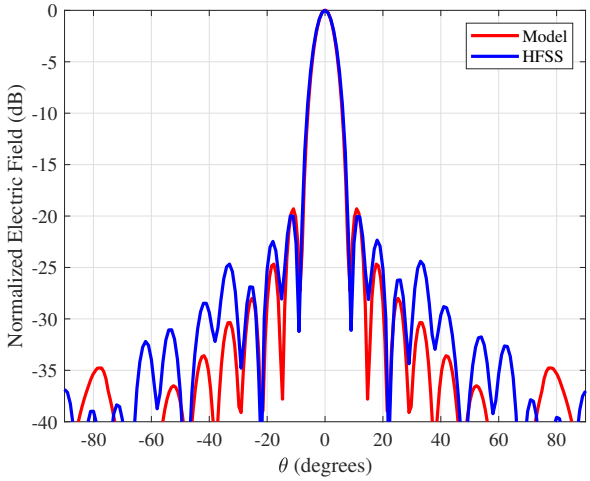

Fig. 6. Normalized NF pattern at $R = 4 \cdot R_{lens}$ of a geodesic lens antenna with $R_{lens} = 4 \cdot \lambda$ and $r_2 = 4 \cdot R_{lens}$.

The following set of parameters was used in the hybrid model: $q = 1.7$, $p = 1$ and $n = 31$. Slight changes to these parameters have limited impact on the numerical results.

A comparison of the FF radiation patterns obtained with the hybrid model and the full-wave simulator is provided Fig. 5. Small differences (less than 0.5 dB) appears in the main beam. The differences increase from angles greater than 20°. However, they are secondary lobes below -20 dB. These discrepancies are mostly due to the real size of the feed (non punctual) and the transition between the lens and the open space (flare), which are not accounted for in the hybrid model.

This antenna is also studied in the NF. The normalized electric field at $R = r_2 = 4 \cdot R_l$, the focusing distance, is illustrated in Fig. 6. The geodesic lens can focus the field within less than 8 degrees (±4°) half-power beamwidth. The differences between the model and the simulation results are very similar to the previous case, with a reasonably good agreement within the main beam and some discrepancies that increase as the side lobe level decreases. Closer to the lens, the main beam widens and the secondary lobes increase. Numerical results are provided for the normalized electric field at $R = 2 \cdot R_l$ in Fig 7.

B. Planar Near Field Analysis

The model allows to study the planar NF distribution of the lens in few seconds. As in the previous section, a geodesic lens with $R_l = 4\lambda$ is studied. The focusing capability of geodesic lenses with $r_2 = 2 \cdot R_l$ and $r_2 = 4 \cdot R_l$ are reported in Fig. 8 and Fig. 9, respectively. In the lens with $r_2 = 2\lambda$, a spot is formed very close to the desired image point. However, in the antenna with $r_2 = 4 \cdot R_l$, a spot of energy appears in a position closer to the lens (around $x = 120$ mm) than expected ($x = r_2 = 160$ mm). This effect is due to the finite dimensions of the lens and also appears in NF planar arrays [24]. The planar NF is also analysed for a Rinehart-Luneburg geodesic lens ($r_2 = \infty$) and the results in amplitude and phase are reported in Fig. 10 and Fig. 11, respectively. As expected, no NF focusing point appears, while the generated plane wave is clearly visible in the phase response.

V. Conclusion

We proposed here a simple model to calculate the FF and the NF of focusing geodesic lenses. The comparison with full-wave simulation results both in the FF and NF validates the proposed approach for the purposes of quick performance assessment (e.g. antenna optimisation, system analyses). This method is used to study the planar NF of this kind of antennas. It is shown that these antennas are able to focus the energy close to the designed position with a precision equivalent to what was demonstrated with planar arrays. These antennas could find applications in short-range

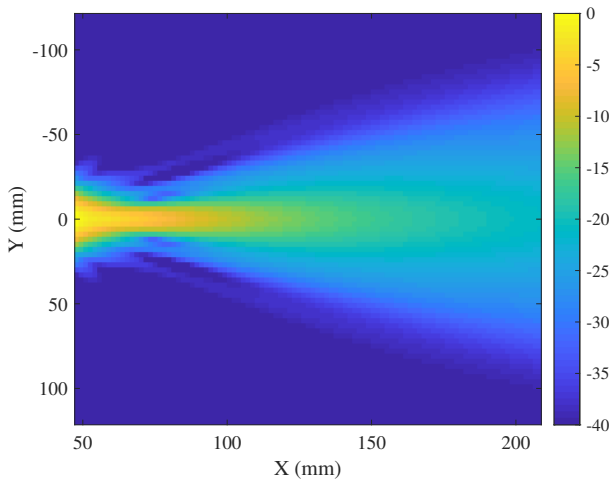

Fig. 8. Normalized planar NF (dB) pattern of a geodesic lens antenna with $R_{lens} = 4 \cdot \lambda$ and $r_2 = 2 \cdot R_{lens}$.

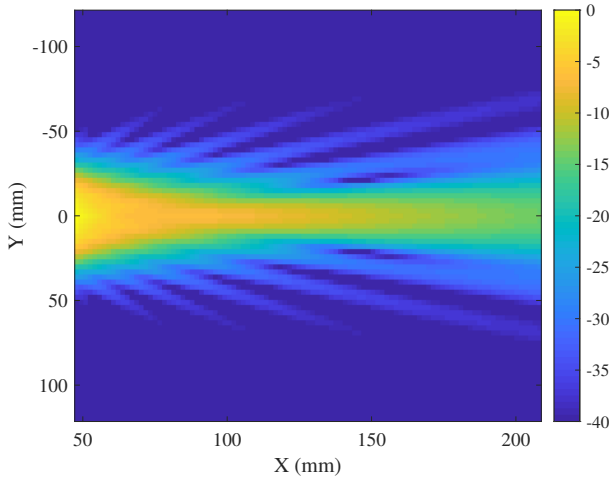

Fig. 9. Normalized planar NF (dB) pattern of a geodesic lens antenna with $R_{lens} = 4 \cdot \lambda$ and $r_2 = 4 \cdot R_{lens}$.

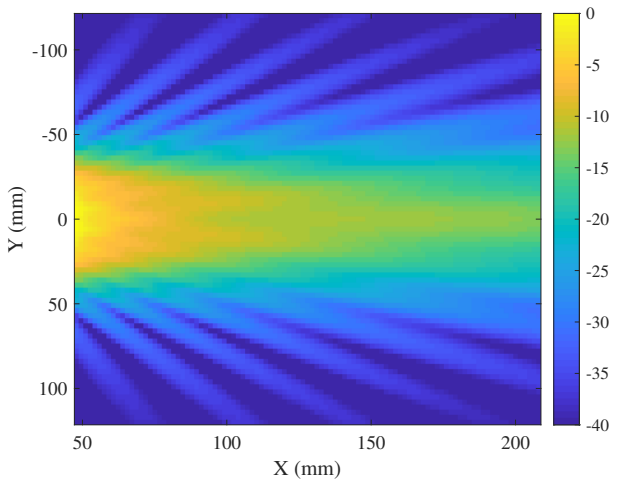

Fig. 10. Normalized planar NF (dB) pattern of a geodesic lens antenna with $R_{lens} = 4 \cdot \lambda$ and $r_2 = \infty$.

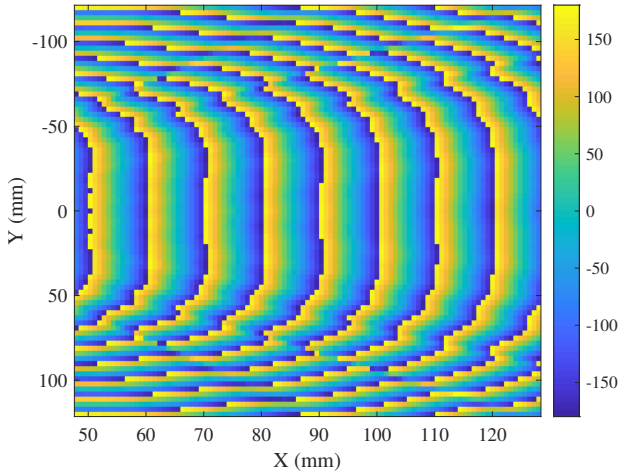

Fig. 11. Phase of the planar NF (degrees) of a geodesic lens antenna with $R_{lens} = 4 \cdot \lambda$ and $r_2 = \infty$.

wireless communications, wireless power transfer or mm-wave imaging sensing systems.

ACKNOWLEDGMENT

This work was supported in part by the Ministerio de Ciencia, Innovación y Universidades, under project TEC2017-86619-R (ARTEINE), the Conserjería de Empleo, Industria y Turismo under project GRUPIN-IDI-2018-000191 and the Swedish VR project 2019-03933 with title High-Spectro.

REFERENCES

[1] N. Fonseca, G. Toso, M. Vorst, P. Jankovic, and P. Angeletti, "Review of lens-based antenna developments supported by ESA for future satellite missions", International Symp. Antennas Propag. (ISAP), Busan, South Korea, 2018.

[2] W. Hong, et al.,"Multibeam Antenna Technologies for 5G Wireless Communications," IEEE Trans. Antennas Propag., vol. 65, no. 12, pp. 6231–6249, Dec 2017.

[3] S. Parkvall, E. Dahlman, A. Furuskar, and M. Frenne, "NR: The new 5G radio access technology", IEEE Commun. Stand. Mag., vol. 1, no. 4,pp. 24–30, Dec. 2017.

[4] O. Quevedo-Teruel, M. Ebrahimpouri and F. Ghasemifard, "Lens Antennas for 5G Communications Systems", IEEE Commun. Mag., vol. 56, no. 7, pp. 36-41, July 2018.

[5] W. Rotman, R. F. Turner, "Wide-angle microwave lens for line source applications," IEEE Trans. Antennas Propag., vol. 11, no. 6, pp. 623-632, Nov. 1963.

[6] W. Lee, J. Kim, and Y. J. Yoon, "Compact two-layer rotman lens-fed microstrip antenna array at 24 GHz," IEEE Trans. Antennas Propag., vol. 59, no. 2, pp. 460–466, Feb. 2011.

[7] K. Tekkouk, M. Ettorre, L. Le Coq, and R. Sauleau, "Multibeam SIW slotted waveguide antenna system fed by a compact dual-layer Rotman lens," IEEE Trans. Antennas Propag., vol. 64, no. 2, pp. 504–514, Feb. 2016.

[8] F. Doucet, N. J. G. Fonseca, E. Girard, H. Legay, R. Sauleau, "Analysis and design of a continuous parallel plate waveguide multiple beam lens antenna at Ku-band," 11th European Conf. Antennas Propag. (EuCAP), Paris, France, pp. 3631-3635, Mar. 2017.

[9] F. Doucet, N.J.G. Fonseca, E. Girard, H. Legay, R. Sauleau, "Analytical

model and study of continuous parallel plate waveguide lens-like multiple beam antennas," IEEE Trans. Antennas Propag., Vol. 66, No. 9, . 4426-4436. Sept. 2018.
[10] N. J. G. Fonseca, "A focal curve design method for Rotman lenses with wider angular scanning range," IEEE Antennas Wirel. Propag. Lett., vol. 16, pp. 54-57, 2017.
[11] R. K. Luneburg. *Mathematical theory of optics*. Providence, Brown University Press, 1944.
[12] C. D. Diallo, E. Girard, H. Legay, and R. Sauleau. "All-metal Ku-band Luneburg lens antenna based on variable parallel plate spacing Fakir bed". 11th European Conf. Antennas Propag. (EuCAP), Paris, France, pp. 1401-1404, Mar. 2017.
[13] O. Quevedo-Teruel, J. Miao, M. Mattsson, A. Algaba-Brazalez, M. Johansson and L. Manholm, "Glide-symmetric fully-metallic Luneburg lens for 5G communications at Ka-band," IEEE Antennas Wireless Propag. Lett., vol. 17, no. 9, pp. 1588-1592, Sept. 2018.
[14] A. Algaba Brazalez, M. Mattsson, L. Manholm, M. Johansson, and O. Quevedo-Teruel, "A Ka-band glide-symmetric planar Luneburg lens with combined dielectric/metasurface for 5G communication", International Symposium on Antennas and Propagation (ISAP), Busan, 2018.
[15] C. Hua, X. Wu, N. Yang, and W. Wu "Air-Filled Parallel-Plate Cylindrical Modified Luneberg Lens Antenna for Multiple-Beam Scanning at Millimeter-Wave Frequencies", IEEE Trans. Microw. Theory Tech., VOL. 61, NO. 1, pp. 436-443. Jan. 2013.
[16] R. F. Rinehart, "A solution of the problem of rapid scanning for radar antennae," J. Appl. Phys., vol. 19, no. 9, pp. 860-862, 1948.
[17] R. F. Rinehart, "A family of designs for rapid scanning radar antennas," in Proc. IRE, vol. 40, pp. 686-688, June 1952.
[18] Q. Liao, N. J. G. Fonseca, O. Quevedo-Teruel, "Compact multibeam fully-metallic geodesic Luneburg lens antenna based on non-Euclidean transformation Optics", IEEE Trans. Antennas Propag., Vol. 66, No. 12, . 7383-7388. Dec. 2018.
[19] N. J. G. Fonseca and O. Quevedo-Teruel, "The water drop lens: a low-profile geodesic parallel plate waveguide lens antenna for space applications," Proc. 13th European Conf. Antennas Propag. (EuCAP), Krakow, Poland, Mar. 2019.
[20] N. J. G. Fonseca, Q. Liao, O. Quevedo-Teruel, "Equivalent planar lens ray tracing model to design modulated geodesic lenses using non euclidian transformation optics", IEEE Trans. Antennas Propag., in press.
[21] M. Šarbort and T. Tyc, "Spherical media and geodesic lenses in geometrical optics," J. Opt, vol. 14, no. 7, p. 075705, 2012.
[22] E. G. Plaza et al., "An ultrathin 2-bit Near-Field transmitarray lens", IEEE Antennas and Wireless Propagation Letters, vol. 16, pp. 1784-1787, 2017.
[23] ANSYS® Electromagnetics Suite , Release 2019 R1, Ansoft Corp., Pittsburgh, PA, USA, 2018.
[24] P. Nepa and A. Buffi, "Near-field-focused microwave antennas: Near-field shaping and implementation", IEEE Antennas and Propagation Magazine, vol. 59, no. 3, pp. 42–53, June 2017.